Journal of Power Sources 273 (2015) 816–822

Contents lists available at ScienceDirect

Journal of Power Sources

journal homepage: www.elsevier.com/locate/jpowsour

Improving cyclic stability of lithium nickel manganese oxide cathode at elevated temperature by using dimethyl phenylphosphonite as electrolyte additive

Shaowei Mai, Mengqing Xu, Xiaolin Liao, Lidan Xing, Weishan Li*

School of Chemistry and Environment, Key Laboratory of Electrochemical Technology on Energy Storage and Power Generation of Guangdong Higher Education Institutes, Engineering Research Center of Materials and Technology for Electrochemical Energy Storage (Ministry of Education), South China Normal University, Guangzhou 510006, China

HIGHLIGHTS

- DMPP is developed as an electrolyte additive for high voltage $LiNi_{0.5}Mn_{1.5}O_4$ cathode.
- DMPP improves significantly cyclic stability of $LiNi_{0.5}Mn_{1.5}O_4$ at elevated temperature.
- Protective film on $LiNi_{0.5}Mn_{1.5}O_4$ is formed due to the preferential oxidation of DMPP.
- Electrolyte decomposition and $LiNi_{0.5}Mn_{1.5}O_4$ destruction is suppressed effectively by DMPP.

ARTICLE INFO

Article history:
Received 4 July 2014
Received in revised form
26 September 2014
Accepted 27 September 2014
Available online 5 October 2014

Keywords:
Dimethyl phenylphosphonite
Electrolyte additive
High voltage cathode
Cyclic stability
Elevated temperature

ABSTRACT

A novel electrolyte additive, dimethyl phenylphosphonite (DMPP), is reported in this paper to be able to improve significantly the cyclic stability of $LiNi_{0.5}Mn_{1.5}O_4$ cathode of high voltage lithium ion battery at elevated temperature. When experiencing charge/discharge cycling at 50 °C with 1C (1C = 146.7 mAh g^{-1}) rate in a standard (STD) electrolyte (1.0 M $LiPF_6$ in ethylene carbonate (EC)/dimethyl carbonate (DMC), EC/DMC = 1/2 in volume), $LiNi_{0.5}Mn_{1.5}O_4$ suffers serious discharge capacity decaying, with a capacity retention of 42% after 100 cycles. With adding 0.5% DMPP into the STD electrolyte, the capacity retention is increased to 91%. This improvement can be ascribed to the preferential oxidation of DMPP to the STD electrolyte and the subsequent formation of a protective film on $LiNi_{0.5}Mn_{1.5}O_4$, which suppresses the electrolyte decomposition and protects $LiNi_{0.5}Mn_{1.5}O_4$ from destruction. Theoretical calculations together with voltammetric analyses demonstrate the preferential oxidation of DMPP and the consequent suppression of electrolyte decomposition, while the observations from scanning electron microscopy, X-ray photoelectronic spectroscopy and Fourier transform infrared spectroscopy confirm the protection that DMPP provides for $LiNi_{0.5}Mn_{1.5}O_4$.

1. Introduction

Lithium ion battery has been widely used as power sources in the field of information technology [1–3], but its energy density needs to be further enhanced for the applications in large scale, such as in the field of electric vehicles. To enhance the energy density of lithium ion battery, much attention has been paid to developing high-voltage cathode materials. $LiNi_{0.5}Mn_{1.5}O_4$ (4.9 V vs. Li/Li^+) is one of the most promising high-voltage cathode materials due to its low cost and non-toxicity [4–7]. However, the cyclic stability of $LiNi_{0.5}Mn_{1.5}O_4$ is poor, especially at elevated temperature, which results from the electrolyte decomposition and the accompanying $LiNi_{0.5}Mn_{1.5}O_4$ destruction [2,3,8].

Several methods have been proposed to inhibit the detrimental reactions on the high-voltage cathode materials, including surface modification of $LiNi_{0.5}Mn_{1.5}O_4$ with inorganic oxides such as ZnO, SiO_2, SnO_2, ZrO_2 and ZrP_2O_7 [9–12] and substitution for carbonates with more stable solvents [13–15]. The surface modification increases the cyclic stability but reduces the specific discharge capacity. Solvents like lactone and sulfone are more stable at 5 V (vs. Li/Li^+) than carbonates, but most of them have high viscosity. Similarly to the protection that electrolyte additives provide for

* Corresponding author. School of Chemistry and Environment, South China Normal University, Guangzhou 510006, China. Tel./fax: +86 20 39310256.
E-mail address: liwsh@scnu.edu.cn (W. Li).

http://dx.doi.org/10.1016/j.jpowsour.2014.09.171
0378-7753/

graphite anode through forming a solid electrolyte interphase (SEI), electrolyte additives have been demonstrated to be able to provide protection for $LiNi_{0.5}Mn_{1.5}O_4$ cathode and thus improve the cyclic stability of $LiNi_{0.5}Mn_{1.5}O_4$ [2,3,16]. Apparently, the strategy of using electrolyte additive is easier to operate and yields less negative effects than other approaches to improve cyclic stability of $LiNi_{0.5}Mn_{1.5}O_4$.

Many factors might affect the protection that electrolyte additives provide for $LiNi_{0.5}Mn_{1.5}O_4$. Among these factors, the molecular structure of the electrolyte additives is most important, which determines the oxidizable ability of the additives and the stability of the formed SEI [16]. To avoid the interference of electrolyte decomposition products, one of which is carbon dioxide, the additives should be oxidized before electrolyte decomposition. On the other hand, the oxidation decomposition products should be robust for forming a stable SEI and are expected to provide SEI with ionic conductivity. Therefore, it is necessary to select electrolyte additives with suitable molecular structure to form an effective SEI.

Phosphorus derivatives have been reported as electrolyte additives for high-voltage cathodes, including trimethyl phosphite (TMP) [17] and triphenyl phosphine (TPP) [18]. TMP was found to be able to improve the cyclic stability and the rate capability of $Li_{1.2}Mn_{0.54}Ni_{0.13}Co_{0.13}O_2$ up to 4.8 V (vs. Li/Li^+), which was attributed to the SEI formed by TMP [17]. The improved rate capability might be related to the oxygen atoms in TMP, which contributes to lithium ion conductivity. However, the oxidation potential of TMP is higher than that of carbonate solvents [17]. TPP was found to be able to improve the cyclic stability of $LiMn_2O_4$ to 4.8 V (vs. Li/Li^+), which was attributed to the insulating film formed by TPP [18]. Compared to TMP, TPP is preferably oxidized (at around 3.68 V, vs. Li/Li^+) and the phenyls in TPP is more robust than alkyls in TMP, and thus facilitates forming more protective film. However, the use of TPP increases the cell resistance due to the insulation of the protective film. In this study, we combined the advantages of TPP and TMP and proposed a novel electrolyte additive, dimethyl phenylphosphonite (DMPP), for improving cyclic stability of $LiNi_{0.5}Mn_{1.5}O_4$. The electrochemical tests and physical characterizations demonstrated that DMPP is an effective additive for the protection of $LiNi_{0.5}Mn_{1.5}O_4$.

2. Experimental

Battery-grade carbonate solvents and lithium hexafluorophosphate ($LiPF_6$) were provided by Guangzhou Tinci Materials Technology Co., Ltd. Dimethyl phenylphosphonite (DMPP) was purchased from Alfa Aesar Technology Co. A standard electrolyte (STD, 1.0 M $LiPF_6$ in ethylene carbonate (EC)/dimethyl carbonate (DMC), EC/DMC = 1/2, in volume) and DMMP as additive were used. The $LiNi_{0.5}Mn_{1.5}O_4$ electrode was prepared by coating a slurry of 80 wt% $LiNi_{0.5}Mn_{1.5}O_4$ (Sichuan Xinneng Advanced Material Co., China), 5 wt% acetylene carbon black, 5 wt% Super-P and 10 wt% PVDF binder on Al foil and dried in vacuum oven. Graphite electrode was prepared for evaluating the effect of DMPP, which was composed of 94.5% natural graphite, 1.0% super-p, 1.5% carboxymethyl cellulose, and 2.0% styrene butadiene rubber.

$Li/LiNi_{0.5}Mn_{1.5}O_4$ coin cells were fabricated in an Ar-filled glove box with prepared electrolytes, $LiNi_{0.5}Mn_{1.5}O_4$ cathode, lithium foil anode and Celgard 2025 separator. In the evaluation of cyclic stability, the cells were charged and discharged with 0.2C (1C = 146.7 mA g^{-1}) at room temperature for two cycles and then with 1C at room temperature or 50 °C for subsequent cycles on LAND test system (CT2001A, China). Li/graphite coin cells were also fabricated and charge/discharge tests were performed with 0.1C (1C = 372 mAh g^{-1}) at room temperature to evaluate the effect of DMPP on the graphite anode.

The linear sweep voltammetry (LSV), cyclic voltammetry (CV) were performed on Solartron-1480 instrument (England). LSV was carried out in an electrolytic cell using platinum disk (100 μm in diameter) as working electrode and lithium foil as both counter and reference electrodes with a scan rate of 5 mV s^{-1}. CV was performed in $Li/LiNi_{0.5}Mn_{1.5}O_4$ coin cells with a scan rate of 0.1 mV s^{-1}. The electrochemical impedance spectroscopy (EIS) measurements were carried out at fully discharged state, the AC perturbation was ±10 mV, and the frequency range was from 10^5 Hz to 10^{-1} Hz on a PGSTAT-302N electrochemical station (Autolab, Metrohm Co., Switzerland).

The cycled cells were disassembled in an Ar-filled glove box, and the cathodes were rinsed with anhydrous DMC to remove residual solvents and $LiPF_6$ salt and dried in vacuum at room temperature. The surface morphology was observed with scanning electron spectroscopy (SEM, JEOL-5900). The surface composition was analyzed with X-ray photoelectron spectroscopy (XPS) on ESCALAB 250 using a focused monochromatized Al K_α radiation ($h\upsilon$ = 1486.6 eV) under ultra high vacuum. The final adjustment of the energy scale was made based on the C 1s peak of graphite at 284.3 eV. The spectra obtained were fitted using XPSPeak 4.1. Lorentzian and Gaussian functions were used for the least-square curve fitting procedure. The organic functional groups in the surface components were characterized by Fourier transform infrared spectroscopy (FTIR) (Bruker Tensor 27) within 600–4000 cm^{-1}.

The energy levels of the highest occupied molecule orbital (HOMO) of the electrolyte solvents and the additive DMPP were calculated by using Gaussian 03 programs package. The equilibrium and transition structures were fully optimized by B3LYP method at 6-31 + G (d, p) basis set.

3. Results and discussion

The use of an electrolyte additive might affect the charge/discharge performance. Fig. 1 presents the charge/discharge profiles of $LiNi_{0.5}Mn_{1.5}O_4$ electrode with 0.2C rate at room temperature between 3.5 and 4.95 V in the STD electrolytes containing various DMPP concentrations. It can be seen from Fig. 1 that increasing DMPP concentration causes the decrease of charge/discharge efficiency: 92.9, 83.2 and 76.9% for the electrolytes containing 0 and 0.5 and 1% DMPP, respectively. This result suggests that DMPP decomposes on $LiNi_{0.5}Mn_{1.5}O_4$ more easily than the STD electrolyte. It can also be noted from Fig. 1 that the discharge capacity is reduced

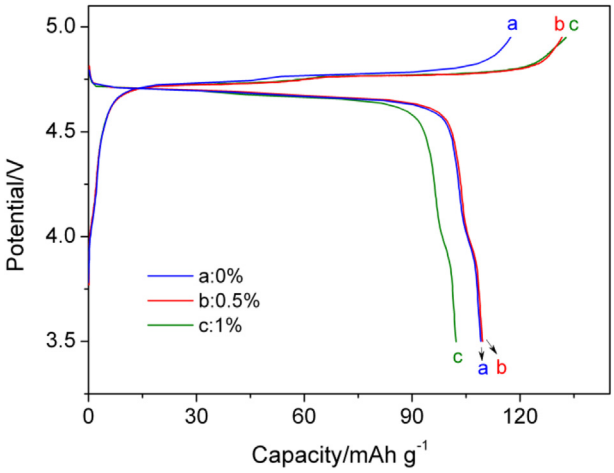

Fig. 1. Charge/discharge profiles of $LiNi_{0.5}Mn_{1.5}O_4$ electrode with 0.2C at room temperature between 3.5 and 4.95 V in STD electrolytes containing various DMPP concentration.

when 1% DMPP is used. This phenomenon might be ascribed to the increased interfacial resistance caused by the subsequent decomposition of DMPP. Therefore, 0.5% DMPP was selected for further investigation in this paper.

Charge/discharge cycling was performed to compare the cyclic stability of $LiNi_{0.5}Mn_{1.5}O_4$ in STD and DMPP-containing electrolytes. Fig. 2 presents the cyclic stability of $LiNi_{0.5}Mn_{1.5}O_4$ in STD and DMPP-containing electrolytes at room temperature with 1C rate between 3.5 and 4.95 V. The discharge capacity of $LiNi_{0.5}Mn_{1.5}O_4$ loses 16.5% in STD electrolyte but remains unchanged in DMPP-containing electrolyte after 145th cycle at room temperature, showing that DMPP can improve the cyclic stability of $LiNi_{0.5}Mn_{1.5}O_4$. It should be noted that the capacity decaying of $LiNi_{0.5}Mn_{1.5}O_4$ in STD electrolyte is not significant at room temperature. However, poor cyclic stability of $LiNi_{0.5}Mn_{1.5}O_4$ would appear at elevated temperature.

Fig. 3 presents the cyclic performances of $LiNi_{0.5}Mn_{1.5}O_4$ in STD and DMPP-containing electrolytes at 50 °C with 1C rate between 3.5 and 4.95 V for 100 cycles. As seen in Fig. 3a, the $LiNi_{0.5}Mn_{1.5}O_4$ cycled in STD electrolyte show a poor cyclic stability, remaining only 42% of its initial capacity after 100 cycles. Without using any additive, the electrolytes tend to decompose on $LiNi_{0.5}Mn_{1.5}O_4$ under high voltage during charging [19] and the transition metal ions (Mn^{4+} and Ni^{4+}) in the delithiated cathode might be reduced by electrolyte to lower oxidation states as Mn^{3+} and Ni^{2+}. The formation of Mn^{3+} might leads to not only the destruction of $LiNi_{0.5}Mn_{1.5}O_4$ due to the Jahn–Teller crystallographic distortion [7] and the dissolution of the transition metal ions from $LiNi_{0.5}Mn_{1.5}O_4$, but also the serious electrolyte decomposition on anode due to the deposition of the dissolved transition metal ions [20]. These negative effects cause the fast decaying of the cell cycled in the standard electrolyte at elevated temperature.

The cyclic stability of $LiNi_{0.5}Mn_{1.5}O_4$ is significantly improved by adding DMPP into the STD electrolyte, as shown in Fig. 3a. The capacity retention is enhanced to 91% after 100 cycles. This result suggests that DMPP can suppress the electrolyte decomposition and protect $LiNi_{0.5}Mn_{1.5}O_4$ from destruction. The selected charge–discharge profiles of the Li/$LiNi_{0.5}Mn_{1.5}O_4$ cells (Fig. 3b and c) show the different variations of polarization with cycling, which is defined as the difference between charge and discharge voltage plateaus. The less increased polarization suggests the better interface stability between $LiNi_{0.5}Mn_{1.5}O_4$ and electrolyte in the cell cycled in additive-containing electrolyte than in STD electrolyte,

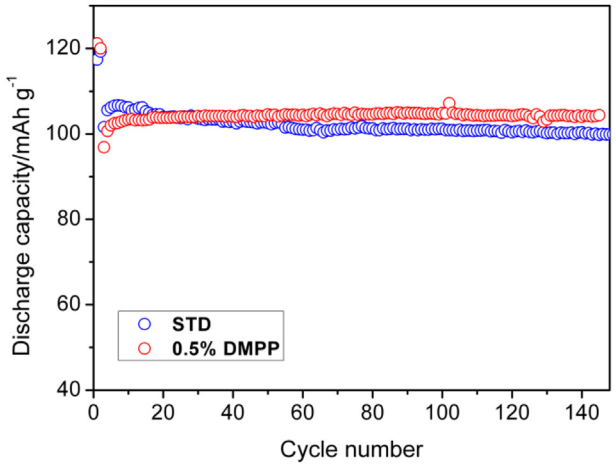

Fig. 2. Cyclic performance of $LiNi_{0.5}Mn_{1.5}O_4$ electrode with 1C at room temperature between 3.5 and 4.95 V.

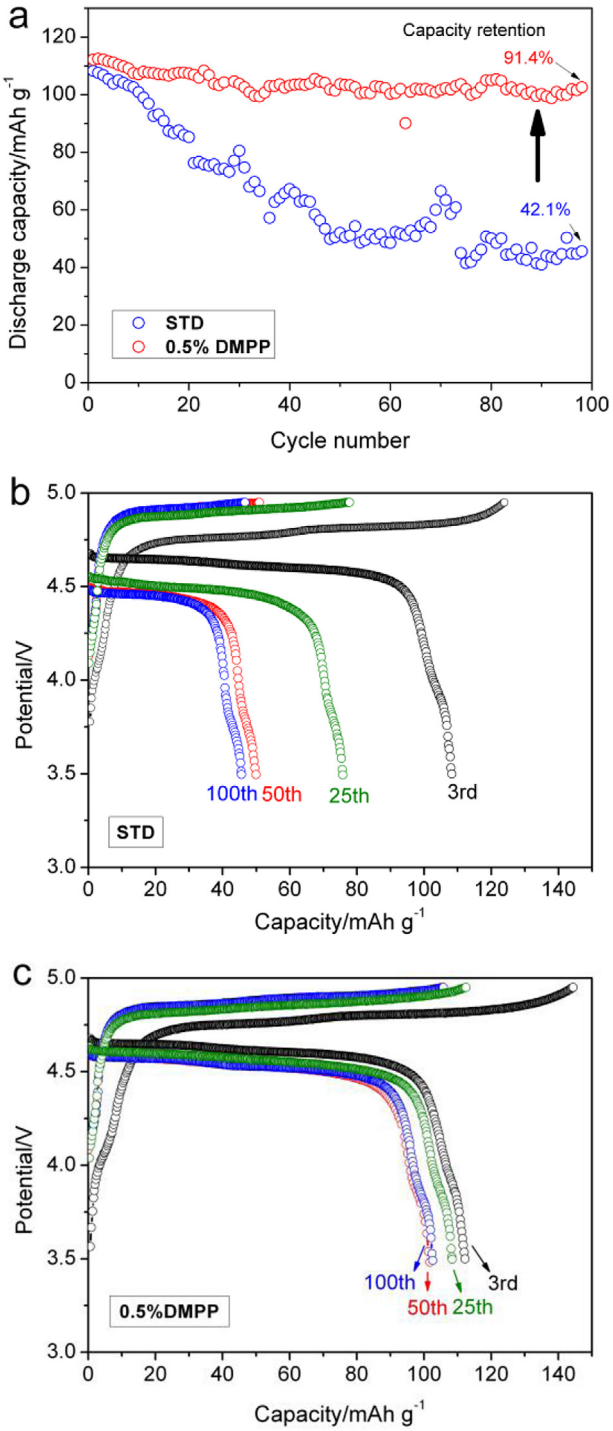

Fig. 3. Cyclic performance of $LiNi_{0.5}Mn_{1.5}O_4$ electrode with 1C at 50 °C between 3.5 and 4.95 V: cyclic stability (a) and charge/discharge profiles of selected cycles in STD (b) and 0.5% DMPP-containing (c) electrolytes.

and confirms the suppression of electrolyte decomposition and the protection of $LiNi_{0.5}Mn_{1.5}O_4$ that DMPP provides.

To understand the mechanism on contribution of DMPP, LSV and CV were used to identify the preferentially oxidative decomposition of DMPP to the standard electrolyte. Fig. 4 presents the voltammograms of platinum electrode in STD and DMPP-containing electrolytes with a scan rate of 5 mV s^{-1}. In the STD electrolyte, the oxidation current appears at about 4.2 V (vs. Li/Li^+) and then

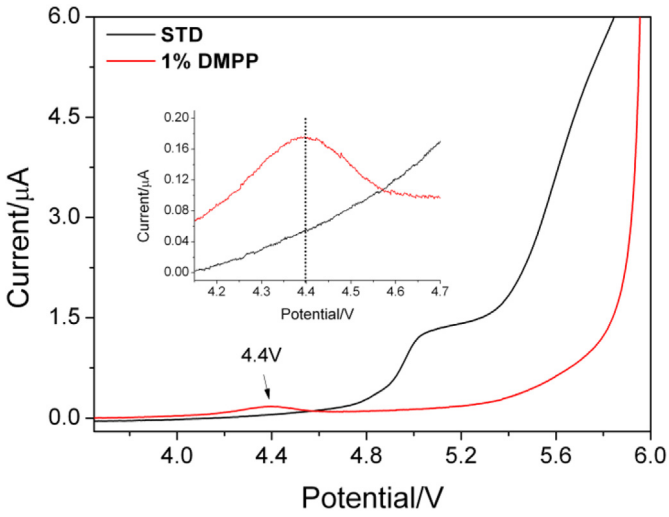

Fig. 4. Linear sweep voltammograms of platinum electrode in STD and 0.5% DMPP-containing electrolytes at a scan rate of 5 mV s^{-1}.

Table 1
HOMO energy of EC, DMC and DMPP.

Organic molecules	HOMO energy (a.u.)
EC	−0.32089
DMC	−0.31080
DMPP	−0.23498

increases slowly from that potential but quickly after 4.6 V. This is a typical characteristic of carbonate electrolyte. Carbonates are instable thermodynamically at the potential above 4.2 V [21] but decompose slowly at the potential up to 4.6 V, which is the reason why current lithium ion battery can be used in practice. The quick decomposition of the carbonate electrolyte at the potential higher than 4.6 V indicates the potential safety issue of high-voltage lithium ion battery. Interestingly, the potential for the decomposition of the STD electrolyte is enhanced to 5.2 V, as shown in Fig. 4, indicative of the suppression of the electrolyte decomposition by using DMPP. As seen in the inset of Fig. 4, the oxidation current on platinum in additive-containing electrolyte is larger than in STD electrolyte at the potential around 4.2 V and an oxidation current peak appears at 4.4 V, indicating that DMPP is oxidized preferentially to the STD electrolyte. Apparently, the suppression of electrolyte decomposition is related to the preferential oxidation of DMPP, which forms a protective film on the electrode. The preferential oxidation of DMPP can be confirmed by theoretical calculations. Table 1 presents the HOMO energies of EC, DMC and DMPP. It can be seen that the HOMO energy of DMPP is higher than that of EC and DMC, confirming the preferable oxidation ability of the additive to the solvents.

Fig. 5 presents the cyclic voltammograms of $LiNi_{0.5}Mn_{1.5}O_4$ electrode in STD and DMPP-containing electrolytes, which were obtained by using a scan rate of 0.1 mV s^{-1}. One pair of redox peaks between 4.5 and 4.9 V can be observed, which are corresponding to the oxidation/reduction of nickel in $LiNi_{0.5}Mn_{1.5}O_4$ [5]. As Fig. 5a shows, the oxidation current between 4.0 and 4.5 V for the electrode in the DMPP-containing electrolyte is larger than that in STD electrolyte, indicating that DMPP is also preferentially oxidized on the $LiNi_{0.5}Mn_{1.5}O_4$ electrode. The smaller current peaks in the initial cycle for the electrode in DMPP-containing electrolyte than that in STD electrolyte (Fig. 5a) indicates that the protective film initially formed by DMPP yields a resistance for lithium ion insertion/extraction. This might be related to the molecular structure of DMPP, which contains phenyls that facilitates the stability but does not contribute to the ionic conductivity of the protective film. Interestingly, the subsequent cycle shows better reversibility (less difference in redox peak potentials) for the electrode in DMPP-containing electrolyte than that in STD electrolyte (Fig. 5b), which is in agreement with the less polarization observed in Fig. 3. This improved reversibility indicates that the protective film formed by DMPP is not a pure insulator but exhibits ionic conductivity to some extent, which can be ascribed to the oxygen atom in DMPP. Therefore, DMPP possesses the advantages of TMP and TPP, the former contributes to ionic conductivity, while the latter to the stability of the protective film, besides the preferential oxidation of TPP.

The variation of the interfacial resistance between $LiNi_{0.5}Mn_{1.5}O_4$ and electrolyte can be confirmed by EIS measurement. Fig. 6 shows the impedance spectra of the $LiNi_{0.5}Mn_{1.5}O_4$ cathodes cycled in STD and DMPP-containing electrolytes. Both cathodes exhibit similar impedance behavior, characteristic of a semicircle and a slope line. The semicircle at high to medium frequencies reflects the interfacial impedance including SEI and charge-transfer resistances, while the slope line at low frequencies is corresponding to the Warburg impedance [22]. The electrode cycled in the DMPP-containing electrolyte shows larger impedance than that cycled in STD electrolyte after initial formation cycles (Fig. 6a), due to the formation of a protective film. However, the electrode cycled in STD electrolyte shows significantly increased interfacial resistance from 2nd to 100th cycle (from 300 to 700 Ω, respectively), indicative of the instability of the $LiNi_{0.5}Mn_{1.5}O_4$/

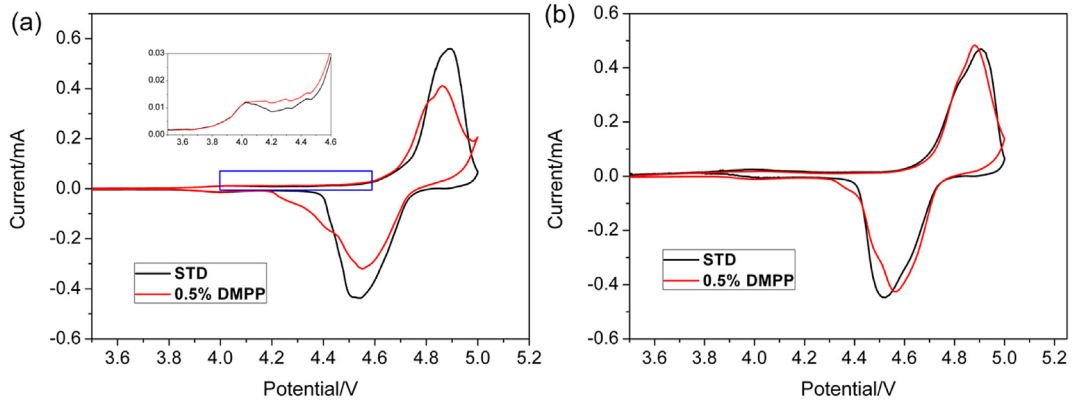

Fig. 5. Cyclic voltammograms of $LiNi_{0.5}Mn_{1.5}O_4$ electrode in STD and 0.5% DMPP-containing electrolytes at a scan rate of 0.1 mV s^{-1}: (a) 1st cycle; (b) 4th cycle.

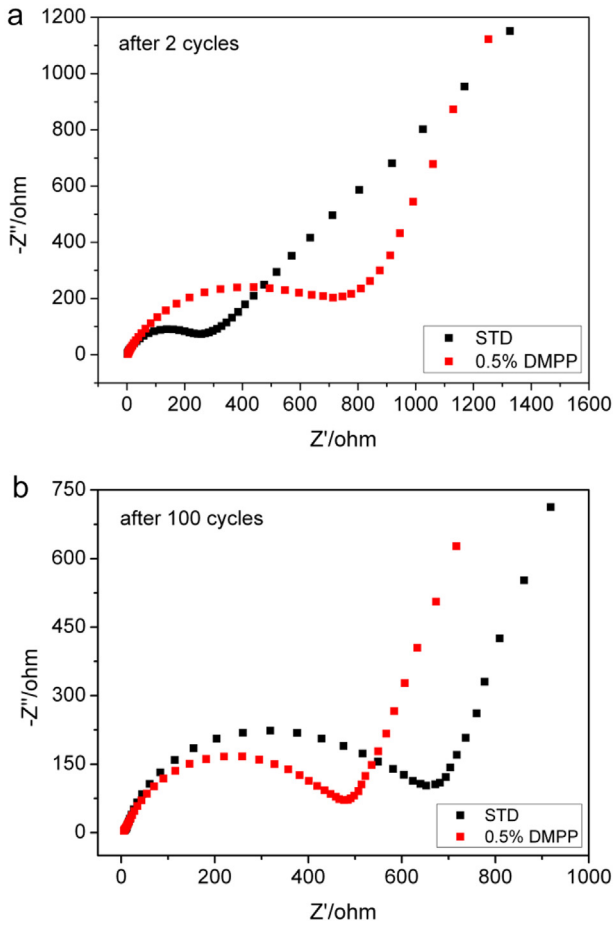

Fig. 6. Electrochemical impedance spectra of $LiNi_{0.5}Mn_{1.5}O_4$ electrode cycled in STD and DMPP-containing electrolytes: (a) after two formation cycles; (b) after 100 cycles.

electrolyte interface due to the electrolyte decomposition and $LiNi_{0.5}Mn_{1.5}O_4$ destruction. Differently, the interfacial resistance of the electrode cycled in the DMPP-containing electrolyte decreases from 700 to 500 Ω after 100 cycles, confirming the improved interfacial stability by DMPP.

To further confirms the contribution of DMPP to the suppression of electrolyte decomposition and the protection of $LiNi_{0.5}Mn_{1.5}O_4$ from destruction, the surface morphology and composition of the cycled $LiNi_{0.5}Mn_{1.5}O_4$ were characterized with SEM, XPS and FTIR.

Fig. 7 presents the SEM images of $LiNi_{0.5}Mn_{1.5}O_4$ electrodes before and after 30 cycles in STD and DMPP-containing electrolytes. The $LiNi_{0.5}Mn_{1.5}O_4$ particles with spinel structure and clean surface can be identified in the pristine electrode, as shown in Fig. 7a. After cycling in the STD electrolyte, crack appears on $LiNi_{0.5}Mn_{1.5}O_4$ particle, as indicated by the arrow in Fig. 7b. The oxidation decomposition of the electrolyte proceeds on the unprotected spinel particles during cycling and is accompanied by the reduction of Mn^{4+} to Mn^{3+}. The formation of Mn^{3+} leads to the destruction of the spinel particle due to the Jahn–Teller crystallographic distortion. Differently, the electrode cycled in the DMPP-containing electrolyte remains its pristine morphology, as shown in Fig. 7c. This observation confirms the protection that DMPP provides for $LiNi_{0.5}Mn_{1.5}O_4$, which results from the protective film formed on $LiNi_{0.5}Mn_{1.5}O_4$ particles due to the preferential oxidation of DMPP.

The fact that DMPP helps form a protective film can be verified by XPS analysis. Fig. 8 shows the C 1s, O 1s, Ni 2p, Mn 2p, Li 1s and P 2p XPS spectra of the $LiNi_{0.5}Mn_{1.5}O_4$ electrodes before and after 30 cycles in STD and TMPP-containing electrolytes. In the C 1s spectra, the peak located at 284.3 eV is assigned to C–C in graphite, and the peaks at 291 and 286.3 eV correspond to C–F in PVDF [2,23]. The weaker peaks for C–C and C–F of the cycled electrode in STD electrolyte than that in DMPP-containing electrolyte indicates that graphite and PVDF is more difficult to detect on the former than the latter, suggesting that thick deposits exist on the former and a thin film is formed on the latter. Besides the peaks observed in the pristine electrode, there appear the peaks corresponding to C–O (286.5 eV), C=O (288 eV) and OCO_2 (289 eV) in the C 1s spectra of the cycled electrodes. These groups can be attributed to $ROCO_2Li$, ROLi and Li_2CO_3 species, which results from the electrolyte

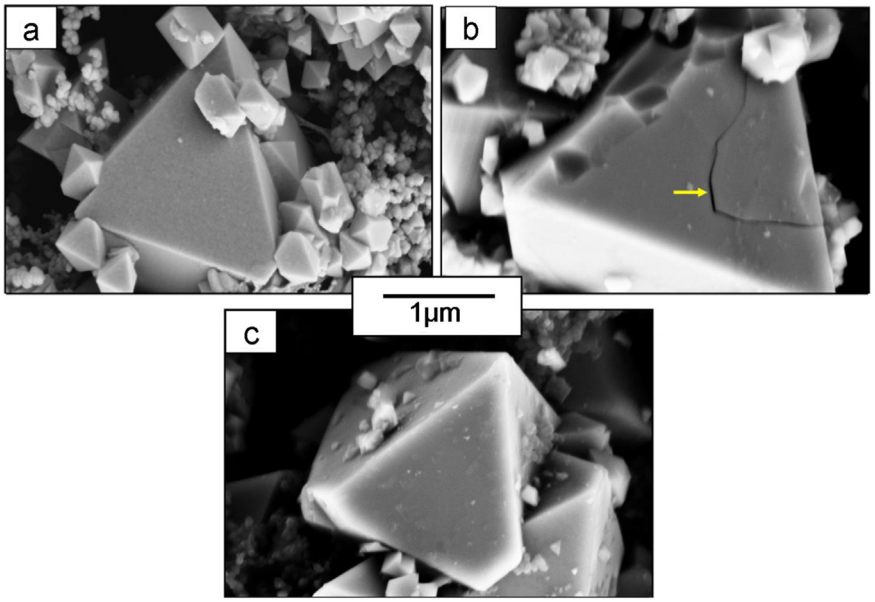

Fig. 7. SEM images of a pristine $LiNi_{0.5}Mn_{1.5}O_4$ electrode (a) and the electrodes after 30 cycles in STD (b) and 0.5% DMPP-containing (c) electrolytes.

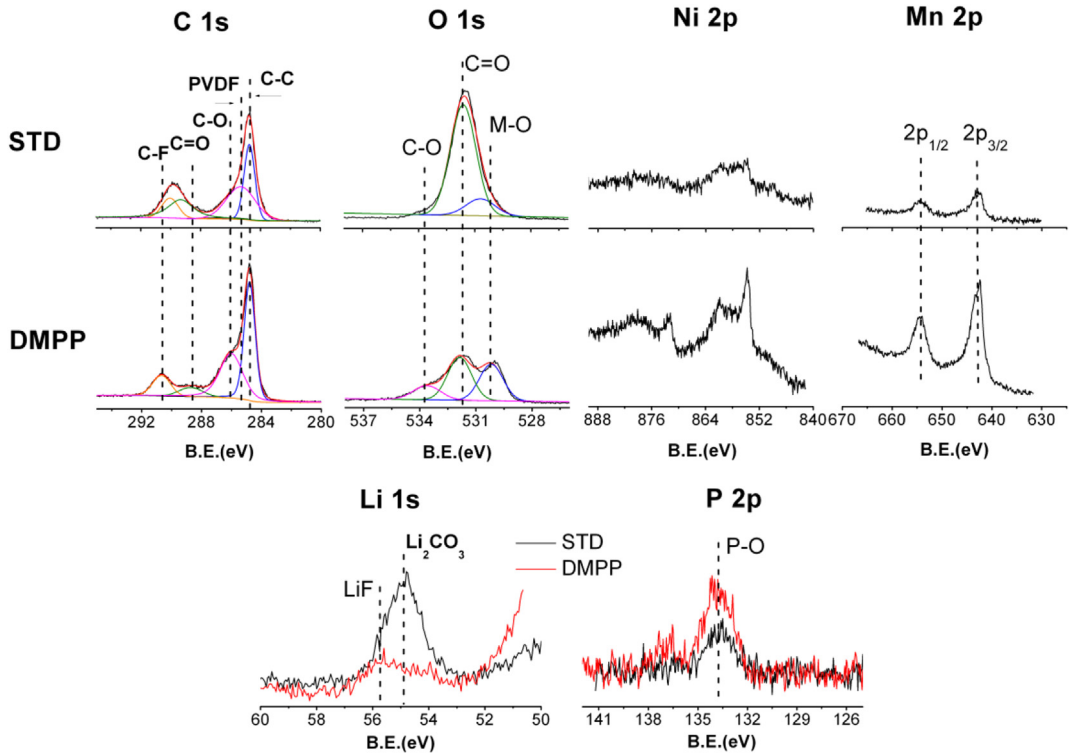

Fig. 8. XPS spectra of $LiNi_{0.5}Mn_{1.5}O_4$ electrodes before and after 30 cycles in STD and DMPP-containing electrolytes.

decomposition on the electrode surface [24–26]. For the O 1s XPS spectra, the peaks are mainly composed of M–O (529.4 eV), C=O (531.2 eV) and C–O (533.3 eV), which are consistent with the presence of metal oxide ($LiNi_{0.5}Mn_{1.5}O_4$), Li_2CO_3/carboxylate/carbonates and ethers [27,28]. The peak of metal oxide for the cycled electrode in STD electrolyte is weaker than that cycled in DMPP-containing electrolyte, confirming the thinner film formed on the $LiNi_{0.5}Mn_{1.5}O_4$ particles by DMPP. In addition, the intensity of C=O peak corresponding to Li_2CO_3 species formed from electrolyte decomposition is much stronger for the cycled electrode in STD electrolyte than that in DMPP-containing electrolyte, confirming that more electrolyte decomposition products exist on the former than the latter. The Li 1s spectra also show that the intensity of Li_2CO_3 species is much stronger for the cycled electrode in STD electrolyte. Moreover, the peak of C–O corresponding to organic ethers appears for the cycled electrode in DMPP-containing electrolyte but cannot be observed for that in STD electrolyte, confirming that the decomposition products of DMPP have been incorporated into the protective film. The P 2p spectra present the P–O peaks for both cycled electrodes. The stronger intensity of P–O peak for the cycled electrode in DMPP-containing electrolyte also confirms that the decomposition products of DMPP have been incorporated into the protective film. The Ni 2p and Mn 2p spectra confirm the above observations that much electrolyte decomposition products exists on the electrode cycled in STD electrolyte while

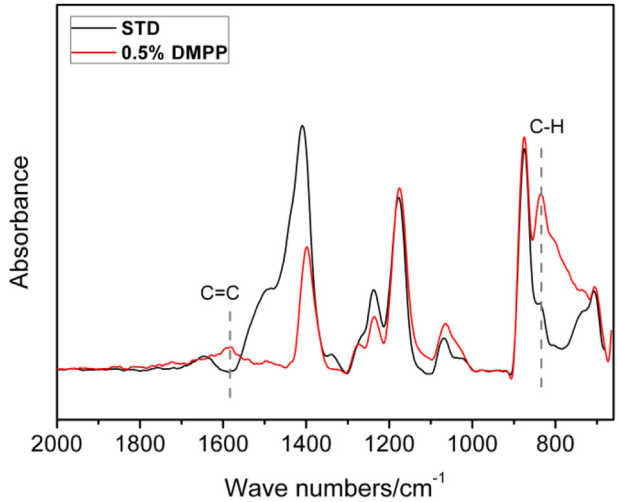

Fig. 9. FTIR spectra of $LiNi_{0.5}Mn_{1.5}O_4$ electrodes cycled in STD and DMPP-containing electrolytes.

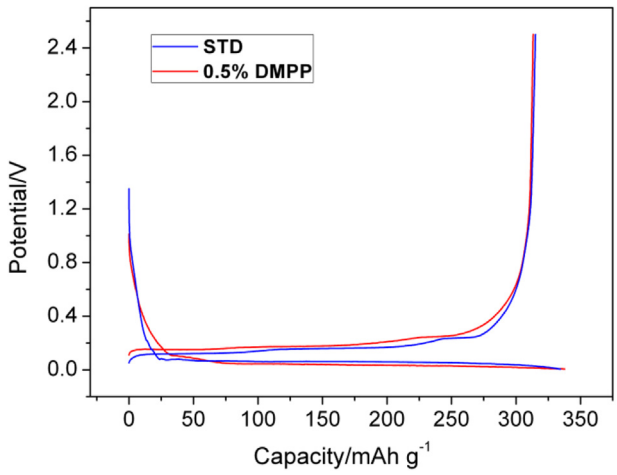

Fig. 10. First charge/discharge profiles of graphite electrode in STD and DMPP-containing electrolytes.

a thin film is formed on $LiNi_{0.5}Mn_{1.5}O_4$ particles in the electrode cycled in DMPP-containing electrolyte.

Fig. 9 compares the FTIR spectra of $LiNi_{0.5}Mn_{1.5}O_4$ electrodes cycled in STD and DMPP-containing electrolytes. The main absorption peaks are predominant by PVDF binder, which is characteristic of the peaks at 1400, 1271, 1175, 1070, 877 and 840 cm^{-1} [29]. Differently from the electrode cycled in STD electrolyte, the electrode cycled in DMPP-containing electrolyte shows additional peaks at 1585 and 834 cm^{-1}, which are characteristic of C=C stretching vibration and C–H bending vibration of benzene. This result confirms that the decomposition products of DMPP have been incorporated into the protective film.

An electrolyte additive used for cathode might yield a negative effect on the anode of lithium ion battery. To understand the effect of DMPP, graphite anode was prepared and performed with charge/discharge test. Fig. 10 presents the initial charge/discharge profiles of graphite anode in STD and DMPP-containing electrolytes. The profile of graphite in DMPP-containing electrolyte is similar to that in STD electrolyte, indicating that DMPP is stable, i.e., DMPP does not yield any negative effect on graphite.

4. Conclusion

Dimethyl phenylphosphonite (DMPP) can be used as an electrolyte additive to improve significantly the cyclic stability of $LiNi_{0.5}Mn_{1.5}O_4$ as cathode of high-voltage lithium ion battery at elevated temperature. DMPP is oxidized preferentially to the electrolyte and helps form a protective film on $LiNi_{0.5}Mn_{1.5}O_4$, which suppresses the electrolyte decomposition and protects $LiNi_{0.5}Mn_{1.5}O_4$ from destruction. Due to the special molecular structure of DMPP, which contains oxygen atoms that might contribute to ionic conductivity and phenyls that might contribute to the stability, the formed film by DMPP is stable and does not yield negative effect, resulting in the significantly improved cyclic stability of $LiNi_{0.5}Mn_{1.5}O_4$.

Acknowledgments

This work is supported by the National Natural Science Foundation of China (21273084 and 21373092), the Joint Project of National Natural Science Foundation of China and Natural Science Foundation of Guangdong (No. U1134002), Natural Science Foundation of Guangdong Province (10351063101000001), the Key Project of Science and Technology in Guangdong Province (Grant No. 2011A010801001), and the Scientific Research Project of Department of Education of Guangdong Province (Grant No. 2013CXZDA013).

References

[1] K. Xu, Chem. Rev. 104 (2004) 4303.
[2] M.Q. Xu, Y.L. Liu, B. Li, W.S. Li, X.P. Li, S.J. Hu, Electrochem. Commun. 18 (2012) 123.
[3] H.B. Rong, M.Q. Xu, L.D. Xing, W.S. Li, J. Power Sources 261 (2014) 148.
[4] M. Hu, X.L. Pang, Z. Zhou, J. Power Sources 273 (2013) 229.
[5] H.B. Lin, Y.M. Zhang, J.N. Hu, Y.T. Wang, L.D. Xing, M.Q. Xu, X.P. Li, W.S. Li, J. Power Sources 257 (2014) 37.
[6] G.Q. Liu, L. Wen, Y.M. Liu, J. Solid State Electrochem. 14 (2010) 2191.
[7] B.Z. Li, L.D. Xing, M.Q. Xu, H.B. Lin, W.S. Li, Electrochem. Commun. 34 (2013) 48.
[8] J.W. Fergus, J. Power Sources 195 (2010) 939.
[9] Y.-K. Sun, K.-J. Hong, J. Prakash, K. Amine, Electrochem. Commun. 4 (2002) 344.
[10] Y. Fan, J.M. Wang, Z. Tang, W.C. He, J.Q. Zhang, Electrochim. Acta 52 (2007) 3870.
[11] R. Santhanam, B. Rambabu, J. Power Sources 195 (2010) 5442.
[12] H.M. Wu, I. Belharouak, A. Abouimrane, Y.K. Sun, K. Amine, J. Power Sources 195 (2010) 2909.
[13] X. Sun, C.A. Angell, Electrochem. Commun. 11 (2009) 1418.
[14] A. Abouimrane, I. Belharouak, K. Amine, Electrochem. Commun. 11 (2009) 1073.
[15] Y.T. Wang, L.D. Xing, W.S. Li, D. Bedrov, J. Phys. Chem. Lett. 4 (2013) 3992.
[16] W.N. Huang, L.D. Xing, Y.T. Wang, M.Q. Xu, W.S. Li, F.C. Xie, S.G. Xia, J. Power Sources 268 (2014) 560.
[17] Z.D. Li, Y.C. Zhang, H.F. Xiang, X.H. Ma, Q.F. Yuan, Q.S. Wang, C.H. Chen, J. Power Sources 240 (2013) 471.
[18] J.J. Xu, Y.Y. Hu, T. Liu, X.D. Wu, Nano Energy 5 (2014) 67.
[19] L.D. Xing, W.S. Li, C.Y. Wang, F.L. Gu, M.Q. Xu, C.L. Tan, J. Yi, J. Phys. Chem. B 113 (2009) 16596.
[20] N. Pieczonka, Z.Y. Liu, P. Lu, K. Olson, J. Moote, B. Powell, J.-H. Kim, J. Phys. Chem. C 117 (2013) 15947.
[21] L.D. Xing, C.Y. Wang, W.S. Li, M.Q. Xu, X.L. Meng, S.F. Zhao, J. Phys. Chem. B 113 (2009) 5181.
[22] D.S. Lu, W.S. Li, X.X. Zuo, Z.Z. Yuan, Q.M. Huang, J. Phys. Chem. C 111 (2007) 12067.
[23] G.C. Yan, X.H. Li, Z.X. Wang, H.J. Guo, C. Wang, J. Power Sources 248 (2014) 1306.
[24] M.Q. Xu, L.S. Hao, Y.L. Liu, W.S. Li, L.D. Xing, B. Li, J. Phys. Chem. C 115 (2011) 6085.
[25] D. Aurbach, I. Weissman, A. Schechter, H. Cohen, Langmuir 12 (1996) 3991.
[26] B. Wang, Q.T. Qu, Q. Xia, Y.P. Wu, X. Li, C.L. Gan, T. van Ree, Electrochim. Acta 54 (2008) 816.
[27] Y.B. Liu, L. Tan, L. Li, J. Power Sources 221 (2013) 90.
[28] M. Xu, L. Zhou, Y. Dong, Y. Chen, A. Garsuch, B.L. Lucht, J. Electrochem. Soc. 160 (2013) A2005.
[29] M.Q. Xu, D.S. Lu, A. Garsuch, B.L. Lucht, J. Electrochem. Soc. 159 (2012) A2130.